Separation and Purification Technology 317 (2023) 123920

Contents lists available at ScienceDirect

Separation and Purification Technology

journal homepage: www.elsevier.com/locate/seppur

# Purification of a monoclonal antibody using a novel high-capacity multimodal cation exchange nonwoven membrane

Jinxin Fan [a,**], Sobhana A. Sripada [a], Dan N. Pham [b], Marina Y. Linova [b], John M. Woodley [b], Stefano Menegatti [a,c,d], Cristiana Boi [a,c,e,*], Ruben G. Carbonell [a,c,f]

[a] Department of Chemical and Biomolecular Engineering, North Carolina State University, Raleigh, NC 27695-7905, USA
[b] Department of Chemical and Biochemical Engineering, Technical University of Denmark, 2800 Kgs Lyngby, Denmark
[c] Golden LEAF Biomanufacturing Training and Education Center (BTEC), North Carolina State University, Raleigh, NC 27695-7905, USA
[d] North Carolina Viral Vector Initiative in Research and Learning (NC-VVIRAL), Raleigh, NC 27695-7905, USA
[e] DICAM, Alma Mater Studiorum – Università di Bologna, 40131 Bologna, Italy
[f] National Institute for Innovation in Manufacturing Biopharmaceuticals (NIIMBL), Newark, DE 19711, USA

ARTICLE INFO

*Keywords:*
Salt-tolerant multimodal ligand
Membrane adsorber
Membrane chromatography
Nonwoven membranes
Monoclonal antibodies (mAbs)
High-risk HCPs

ABSTRACT

A high-capacity, multimodal cation exchange (MMC) chromatographic membrane was developed by conjugating a multimodal ligand – 2-mercaptopyridine-3-carboxylic acid (MPCA) – on a polybutylene terepthalate (PBT) nonwoven fabric. The membrane features an equilibrium binding capacity of ≈ 1000 mg of human polyclonal IgG (IgG) per g of membrane and dynamic binding capacities ($DBC_{10\%}$) ranging from 77.5 to 115.1 mg/mL (residence times of 1 and 5 min, respectively); these values are 2-to-3-fold higher than those of commercial MMC adsorbents. The effects of buffer composition, pH, conductivity on the binding behavior of the MMC-MPCA membrane were investigated in detail. As a moderate cation exchange binder, MPCA enables effective protein elution using buffers with mild pH (8.0–9.0) and conductivity (≈13 mS/cm), thus circumventing the harsh conditions often needed in multimodal chromatography. The MMC-MPCA membrane was evaluated for product capture in bind-and-elute mode on a Chinese hamster ovary (CHO) cell culture harvest containing therapeutic monoclonal antibodies, using commercial multimodal (Capto MMC and MX-Trp-650M) and affinity (AF-rProtein A HC-650F) resins as controls. The MMC-MPCA membrane outperformed the multimodal resins in terms of binding capacity as well as clearance of host cell proteins (HCPs) and aggregates. The membrane was then evaluated by polishing the mAb from a Protein A eluate in bind-and-elute mode. The MMC-MPCA membrane reduced the level of high molecular weight components from 11% to 4% and the HCP content from 1319.7 ppm to 48.7 ppm (LRV of 1.4). Most notably, proteomics analysis of the product demonstrated the clearance of a significant fraction of persistent, high-risk HCPs from the Protein A eluate.

## 1. Introduction

With the growing demand for accessible biotherapeutics, the accelerating emergence of novel therapeutic modalities, and increasing competition from biosimilars, the biopharmaceutical industry is seeking to transform manufacturing processes to increase productivity, flexibility, and adaptability to different products and scales, while reducing costs and time to market [1–3]. Therapeutic monoclonal antibodies (mAbs) remain the dominant class of biopharmaceuticals in terms of production volume and variety of applications. With downstream processing accounting for over 50% of mAb production costs [4,5], significant efforts are devoted to the development of compact and affordable purification processes [6]. In this context, a key role is played by innovating chromatographic technologies [7], particularly the design of novel ligands with improved separation orthogonality and novel substrates that grants high flowrate operations.

On the front of ligand chemistry, special attention is dedicated to multimodal ligands (*e.g.*, Capto™ Adhere and MEP HyperCel™), that combine hydrophobic, hydrogen binding and electrostatic interactions and provide orthogonal separation mechanisms, complementing the

* Corresponding author at: DICAM, Alma Mater Studiorum – Università di Bologna, 40131 Bologna, Italy (C. Boi).
** Co-corresponding author at: Department of Chemical and Biomolecular Engineering, North Carolina State University, Raleigh, NC 27695-7905, USA (J. Fan).
*E-mail addresses:* jfan22@ncsu.edu (J. Fan), cristiana.boi@unibo.it (C. Boi).

https://doi.org/10.1016/j.seppur.2023.123920
Received 14 March 2023; Received in revised form 19 April 2023; Accepted 20 April 2023
Available online 25 April 2023

affinity or the conventional ion exchange or hydrophobic chromatography [8–11]. Many multimodal ligands exhibit a salt-tolerant character, where the binding capacity is relatively independent of solution conductivity [12,13]. Salt tolerance reduces the need for buffer exchange or dilution to adjust pH and conductivity, enabling significant reductions in operating costs and processing time [7,12]. Moreover, multimodal chromatography has been found to be effective in the removal of product- and process-related impurities – such as aggregates, protein fragments, host cell proteins (HCPs) and DNA – following the mAb product capture step by Protein A chromatography [5,8,11]. For instance, Zhang *et al.* demonstrated that multimodal cation exchange chromatography employed in bind-and-elute mode can successfully isolate mAb monomers from aggregates [5]. An additional advantage of multimodal chromatography is the ability to capture the product directly from unconditioned recombinant fluids [14,15]. For example, MEP HyperCel™ has been used to capture full mAbs and single-chain fragments from cell culture fluids [16,17]. These applications are being considered as effective alternatives to the expensive, and less stable, Protein A and protein L chromatography for the purification of whole antibodies and Fab fragments [16,18].

On the front of novel substrates, membranes are emerging as a viable alternative to resins to increase productivity and flexibility. While characterized by lower surface areas per unit volume and hence lower binding capacity than chromatographic resins, membranes have much larger flow permeabilities and their dynamic binding capacity is essentially independent of flow rate due to the absence of diffusional limitations. This allows membrane adsorbers to operate at a much shorter residence times, thus increasing productivity [19,20]. With recent developments in surface chemistry and fabrication techniques leading to higher binding capacities and opening the route to affordable single-use (or disposable) devices, membranes are poised to acquire a preeminent role in downstream bioprocessing [2,21,22].

It is therefore surprising that there has been little work reported on the use of multimodal ligands in membrane chromatography. Ma *et al.* screened four multimodal ligands including 2-mercaptobenzimidazole, 2-mercapto-1-methylimidazole, 2-mercaptopyridine, and 4-mercaptopyridine on a cast microporous regenerated cellulose membrane support modified by the ring-opening polymerization of diethylene glycol diglycidyl ether [23]. The 2-mercaptobenzimidazole ligand membrane had a high dynamic binding capacity (DBC) of 65 mg/mL of membrane for human polyclonal IgG at a residence time of 0.1 min. Wang *et al.* developed a salt-tolerant cation exchange membrane, also based on a cast porous regenerated cellulose membrane, but with 4-mercaptobenzoic acid as ligand [13]. This membrane had a DBC of 38–47 mg IgG/mL at NaCl concentrations from 0 to 150 mM and residence times shorter than 0.1 min [13]. However, the strong hydrophobic binding by the phenyl and benzimidazole rings of these ligands combined with the high ligand densities required elution from both membranes to be conducted at low pH (pH 2.5) and high concentrations of chaotropic salt (*e.g.*, sodium isothiocyanate) [13,23]. Such harsh elution conditions raise the risk of aggregate formation and mandates rapid buffer exchange of the eluates (lower the salt concentration or increase pH) to curb product degradation [24,25].

In this work, we developed a multimodal salt tolerant cation exchange membrane by coupling 2-mercaptopyridine-3-carboxylic acid (MPCA) to a polybutylene terephthalate (PBT) nonwoven fabric modified by UV grafting of glycicyl methacrylate (polyGMA) [26,27]. Nonwoven fabrics offer great promise as disposable chromatographic membranes owing to their low pressure drops at high flow rates, affordable scalability, flexible and rapid production as well as high binding capacity after functionalization with ligands [2,28]. To our knowledge, this is the first work on the preparation of multimodal membranes based on nonwoven fabrics and the use of such membranes for product capture and product polishing in the purification of biotherapeutics. The same MPCA ligand, has been linked to vinylsulphone-activated agarose gel and nanoparticles in previous studies obtaining a low IgG binding of 3–4 mg/mL in the isolation of IgG from human serum via thiophilic interactions [29,30]. In our study, MPCA is conjugated on the membrane by reaction with the epoxy group in the polyGMA and the purification mechanism is mainly reliant on charge-charge interactions. The resulting multimodal cation exchange membrane (MMC-MPCA) was characterized in terms of equilibrium and dynamic binding capacity for human IgG at a variety of residence times, and reusability over multiple cycles. The binding mechanism between the ligand and IgG was investigated by studying the effects of buffer pH, composition, and concentration (conductivity) on protein binding and elution. The membrane's separation performance was tested by purifying a monoclonal antibody (mAb) from a clarified CHO cell supernatant using two different methods: (1) as a product capture membrane, and (2) as a bind-and-elute polishing step following a Protein A column. The results obtained for mAb capture with the membrane were compared with the results using one affinity Protein A resin (AF-rProtein A HC-650F) and two commercial multimodal ligand resins (Capto MMC and MX-Trp-650M) under similar conditions. Proteomic analysis of the polished product was carried out to evaluate the ability of the membrane to reduce the level of high-risk host cell proteins co-eluting with the mAb from the Protein A resin.

## 2. Experimental

### 2.1. Materials

Poly(butylene terephthalate) (PBT) nonwoven membranes (basis weight 52 g/m$^2$, mean fiber diameter 3.0 μm, 85% porosity, and mean pore size 8.0 ± 0.5 μm) were provided by Macopharma (Tourcoing, France). Glycidyl methacrylate (GMA) was purchased from Reagent World (Ontario, CA, USA). Benzophenone (BP) and MPCA were purchased from Sigma-Aldrich (St. Louis, MO, USA). The organic solvents used for membrane preparation and chemicals for buffer preparation were purchased from Fisher Scientific (Fairlawn, NJ, USA). Human polyclonal IgG (IgG) was purchased from Athens Research & Technology, Inc. (Athens, GA, USA). Capto MMC resin and 5 mm-diameter columns to pack chromatographic resin particles were purchased from Cytiva (Marlborough, MA, USA). The MX-Trp-650M resin and AF-rProtein A HC-650F resin were purchased from Tosoh (Tokyo, Japan). The CHO supernatant (2.2 mg/mL mAb, ~0.66 mg/mL HCPs, pH 7.5) was generously provided by Fujifilm Diosynth Biotechnologies (Durham, NC, USA). The ratio of HCP to product is 0.3 mg HCP/mg of mAb, which in parts per million (ppm) of HCP per mass of mAb corresponds to 3 × 10$^5$ ng/mg.

### 2.2. Preparation of MMC-MPCA membrane

UV grafting of GMA on PBT nonwoven was conducted using the procedures described in previous publications [26,28]. The grafting time was adjusted to obtain different GMA degrees of grafting, as measured by the percentage weight gain (WG) of the original PBT sample:

$$\mathrm{WG}(\%) = \frac{W_1 - W_0}{W_o} \times 100\% \quad (1)$$

Wherein $W_0$ is the weight (g) of the original PBT sample and $W_1$ is the membrane weight (g) after UV grafting of GMA. Grafting times of 14–22 min were employed to obtain weight gains in the range of 11.5%–25%.

PolyGMA grafted PBT samples (17–18% WG, average 17.5% WG) were soaked in MPCA solutions for ligand coupling at 60 °C in a water bath for 16 h. The solutions contained 0.5–20 mg MPCA/mL, corresponding to molar ratio of epoxy/MPCA of 1:0.5–1:21.5. This step was followed by 0.1 M sulfuric acid treatment at 50 °C for 16 h to hydrolyze unreacted epoxy groups in the polyGMA. The prepared cation exchange MPCA membranes (MMC-MPCA) were washed three times with pure water. The optimal molar ratio of epoxy/MPCA was determined by

measuring the dynamic binding capacity of the membranes for IgG at 10% breakthrough ($DBC_{10\%}$) (method described in Section 2.4.2). Once the optimal epoxy/MPCA ratio was determined, the GMA grafting degree (11.5%–25%) was then optimized to obtain MMC-MPCA membranes with the highest protein $DBC_{10\%}$.

### 2.3. Membrane characterization

The ligand density was determined by quantifying the sulfur content of the modified MPCA nonwoven membrane with a PE 2400 CHN elemental analyzer (PerkinElmer Inc., Waltham, MA, USA). The membrane zeta potential at pH 2.5–11.0 was measured with a SurPASS 3 electrokinetic analyzer (Anton Paar, Graz, Austria). For flow permeability measurements, 50 layers of MMC-MPCA membrane were packed into an Omnifit column of 1.0 cm diameter from Diba Industries, Inc. (Cambridge, UK). The resulting membrane bed height for these flow experiments was 1.3 cm (1.0 mL column volume) and the column pressure was measured at various flow rates using an ÄKTA™ pure system (Marlborough, MA, USA) using 50 mM acetate buffer pH 5.5 as the mobile phase with superficial velocities ranging from 229.2 to 763.9 cm/h (corresponding to 0.1–0.33 min RT). The pressure drop $\Delta P$ across the membrane layers (kPa) was estimated by subtracting the pressure drop of the empty column from that of column with the membranes to get a pressure drop per unit bed length ($\Delta P/L$) where $L$ is the height of membrane packed bed (cm). The flow permeability of the membrane was calculated using Darcy's law:

$$v = k\frac{\Delta P}{\mu L} \tag{2}$$

Where $v$ is the superficial velocity in the column and $\mu$ is the viscosity of the aqueous solution.

### 2.4. Membrane performance for protein binding and elution

#### 2.4.1. Equilibrium binding capacities and isotherm for human IgG

The equilibrium binding capacity of the membrane was measured by immersing 15 mg membrane samples in 3.0 mL 50 mM acetate buffer pH 5.5 with 150 mM NaCl (hereafter referred as binding buffer) containing human IgG for 16 h at room temperature. The binding capacity was calculated as the mass of bound protein (the difference of protein mass in the solution before and after incubation) divided by the weight of the membrane. A range of IgG initial concentrations from 0.5 to 12.5 mg/mL for binding experiments was employed for studying the equilibrium adsorption isotherm. The Langmuir isotherm was used to fit the experimental adsorption data:

$$q_{eq} = \frac{q_m c_{eq}}{c_{eq} + K_d} \tag{3}$$

Wherein $q_{eq}$ is the measured amount of IgG adsorbed on the membrane at equilibrium while $c_{eq}$ is the IgG concentration in solution at equilibrium. The values of the Langmuir parameters, $q_m$, the maximum binding capacity, and $K_d$, the dissociation constant, were determined by fitting the experimental data using Eq. (3). The same procedure was used for measuring the adsorbed IgG on the membrane in different buffers (adjusting 50 mM acetate pH 5.5 with 1.0 M NaOH, 1.0 M HCl and other salts), for investigating the influence of pH (4.5–7.0 with added 150 mM NaCl), salt concentration (0–450 mM NaCl), and salt type (50 and 150 mM NaCl, NaCitrate, $Na_2SO_4$, $MgCl_2$) on protein adsorption. The initial IgG concentration of IgG binding studies using the above buffers was 5.0 mg/mL.

Elution was also conducted at a variety of conditions: 50 mM acetate pH 5.5 with 1.0–2.0 M NaCl, 1.0–2.0 M urea, 20%-30% (v/v) ethylene glycol, 0.2–1.5 M arginine, 50 mM phosphate buffer pH 8.0 with 0–1.5 M NaCl and 50 mM carbonate buffer pH 9.0 with 150 mM NaCl. The elution efficiency was calculated as the mass ratio of the eluted protein to the bound protein.

#### 2.4.2. Dynamic binding capacities for IgG

The membrane dynamic binding capacity for IgG at 10% breakthrough ($DBC_{10\%}$) was measured in flow experiments with 12 membrane layers (≈0.24 mL) packed in the 1.0 cm diameter Omnifit column holder mentioned earlier using the ÄKTA™ pure system. The membranes were equilibrated with 7.2 mL of binding buffer at 0.5 mL/min. Then 3 mg IgG/mL sample solutions were loaded at residence time (RT) of 1.0, 2.0, or 5.0 min. The loading process was stopped once the UV absorbance reached the value corresponding to 10% of the initial feed concentration. An elution buffer consisting of 7.2 mL of 50 mM carbonate buffer pH 9.0 with 150 mM NaCl was applied at a flow rate of 0.5 mL/min, if membrane reuse was needed. The $DBC_{10\%}$ was calculated as follows:

$$DBC_{10\%} = \frac{c_0(V_{10\%} - V_0)}{V_m} \tag{4}$$

Wherein $c_0$ is the initial IgG concentration in the feed (mg/mL); $V_{10\%}$ is the effluent volume when the IgG concentration in the effluent reached 10% of the initial IgG concentration in the feed (mL); $V_0$ is the void volume (mL), determined in separate experiments using a pulse of 2% acetone, and $V_m$ is the membrane volume.

### 2.5. mAb purification from cell culture supernatant in bind-and-elute mode

#### 2.5.1. Product capture mode

The MMC-MPCA membrane was used for direct capture of a mAb from a CHO cell culture supernatant and the results were compared with those obtained using commercial cation exchange resins (Capto MMC, MX-Trp 650 M) and a Protein A resin (AF-rProtein A HC-650). The membranes were packed in the 1.0 cm diameter Omnifit column as described above, while the multimodal Capto MMC, and the MX-Trp 650 M resins were packed in 5.0 mm diameter columns to bed volumes of 0.24–0.25 mL, so that both resins and membrane column volumes were identical. Before the capture experiments, the pH of the CHO supernatant was adjusted to pH 5.5 or pH 4.5 depending on the media, followed by filtration with a 0.22 μm membrane. The filtered solution was used as feedstock. In the separations using Capto MMC, MX-Trp 650 M and MMC-MPCA, 6.0 mL of feed solution (≈11 mS/cm) were injected at 5.0 min RT after column equilibration by 12.5 mL 50 mM acetate buffer pH 5.5 with added 90 mM NaCl (≈11 mS/cm). After sample loading, the same equilibration buffers were used for washing until the UV absorbance returned to baseline. Finally, the bound protein was eluted by 7.5 mL 50 mM carbonate buffer with additional 150 mM NaCl at pH 9.0 (≈17 mS/cm). The equilibration, washing, and elution steps for the MMC-MPCA membrane were all conducted at 0.5 min RT, while for the resins the RT in all these steps was 5.0 min. A 0.1 M arginine wash step was used in one of the MMC-MPCA runs to determine its potential use to improve HCP removal in the eluate. For the Protein A resin, the 2.0 mL AF-rProtein A HC-650F column was equilibrated with 20 mL phosphate buffered saline (PBS, pH 7.4), followed by loading with 30 mL clarified supernatant without any adjustment using 5.0 min RT. After washing with 30 mL PBS, the bound protein was eluted by 10 mL of 0.1 M citric acid at pH 3.0. The eluate was neutralized by 1.0 M Tris-HCl buffer at pH 8.0 immediately after elution was completed. The equilibration, washing and elution steps in Protein A chromatography were processed at 2.0 min RT. The DBC during purification was calculated as the mass of the eluted mAb divided by the volume of membrane or resin. Recovery was calculated as the mass ratio of the eluted mAb to the mAb in the loading solution.

The mAb concentrations, HCP concentration and aggregate contents were measured respectively via analytical Protein G chromatography, ELISA, and analytical size exclusion chromatography (SEC-HPLC), using methods described in a prior publication [28]. A Yarra SEC-2000 size exclusion chromatography column (300 mm × 7.8 mm) purchased from Phenomenex Inc. (Torrance, CA, USA) was used for analyzing mAb

aggregates. The Waters Alliance 2690 separation module system and Waters 2487 dual absorbance detector for HPLC analysis were purchased from Waters Corporation, Milford, MA, USA. The CHO HCP ELISA Kit (F550) was obtained from Cygnus (Southport, NC, USA).

#### 2.5.2. Polishing a protein A eluate in bind-and-elute mode

The MMC-MPCA membrane was used to polish a Protein A eluate obtained by feeding the mAb supernatant as described in Section 2.5.1. The eluate from the Protein A column was immediately adjusted to pH 5.5 by adding 1.0 M pH 8.0 Tris-HCl and the solution was filtered by 0.22 μm membrane before loading to the MMC-MPCA membrane that was used for the polishing step. The chromatographic procedure was the same as that used in the product capture studies above except for loading 2.0 mL feed solution. After elution, the membrane was regenerated with 7.5 mL 2.0 M guanidine-HCl and then washed with 12.5 mL 50 mM acetate buffer pH 5.5.

### 2.6. Proteomic analysis

Proteomic analysis was performed to identify and track HCPs, including problematic HCPs, which could be deleterious to the product or cause human immunogenic responses. Samples of the CHO supernatant, the Protein A column eluate, and MMC-MPCA membrane eluate were analyzed. These samples were treated with trypsin for digestion according to our prior work [31,32], followed by washing with 50 mM ammonium bicarbonate, drying, and reconstituting in 1 mL aqueous 2% v/v acetonitrile, 0.1% v/v formic acid (mobile phase A). The samples were then diluted 1:5 in mobile phase A before injection. Proteomics analysis by nano LCMS/MS using the method reported in [32] at the Molecular Education, Technology, and Research Innovation Center (METRIC) at NC State University. The resulting nano LC-MS/MS data were processed with Proteome Discoverer 2.4 (Thermo Fisher, San Jose, CA). The abundance values reported by Proteome Discoverer post evaluating a match between runs were used to calculate intra-sample relative abundance and derive inter-sample label-free quantification analyses after the exclusion of the identified contaminant species (Porcine Trypsin, Keratin).

## 3. Results and discussion

### 3.1. MMC-MPCA membrane equilibrium and dynamic binding capacities for IgG

Our strategy for ligand conjugation begins with grafting brushes of poly(glycidyl methacrylate) (polyGMA) on the fibers of a polybutylene terephthalate (PBT) nonwoven fabric [26,28]: the epoxy ring of GMA reacts with the thiol group displayed by the ligand – herein, 2-mercaptopyridine-3-carboxylic acid (MPCA) – forming a stable thioether bond (Fig. 1; *note:* unreacted epoxy rings are converted to hydroxyl groups via hydrolysis with 0.1 M sulfuric acid). As demonstrated previously with other ligands, the degree of GMA grafting, was measured by the % weight gain (%WG) upon grafting, and the ligand concentration used during conjugation determine ligand density on the membrane and thus its protein binding capacity [28]. Accordingly, two conditions were adjusted to obtain a ligand density that promotes protein binding on the MMC-MPCA membrane. Following estimation of the available epoxy groups based on the %WG, the molar ratio of MPCA/epoxy during conjugation was varied to determine its effect on ligand density and dynamic binding capacity ($DBC_{10\%}$). Fig. 2 shows that a grafting WG of 17.5% and an epoxy/MPCA ratio of 1:2.2 led to the highest values of IgG $DBC_{10\%}$ (77.5 mg/mL at of 1.0 min RT). Notably, this membrane featured an intermediate value of ligand density (0.42 μmol/mg), consistent with most observations in the literature: higher ligand density, in fact, tends to crowd out the target proteins, while low ligand densities offer insufficient binding sites, both resulting in lower capacities [33–35]. The remainder of this study was conducted using membranes prepared under these optimized conditions.

The selected membrane was then evaluated via equilibrium adsorption studies using a panel of IgG solutions with concentrations varying from 0.2 to 12.5 mg/mL (Fig. 3). The resulting isotherm adsorption curve fits well the Langmuir model in Eq. (3), returning a calculated maximum adsorption capacity $q_m$ of ≈1000 mg/g of membrane, corresponding to 312.2 mg/mL of dry membrane, and a $K_d$ of 1.55 mg/mL (10.3 μM). The value of binding capacity is much higher than those of multimodal cation exchange resins and membranes reported in the literature [13,23,36], and is rooted in the ligand-functionalized grafted brushes, which form a 2500 Å-thick layer around the 3 μm-diameter fibers. The grafted layers consist of expandable, polymer networks that allow penetration of the proteins, so that the binding does not rely solely on the surface area of the fiber. The membrane used in these studies has a measured intrinsic surface area of about 1 $m^2/g$ of fabric. A monolayer of proteins adsorbed to the surface of the fibers would result in, at most, 5–6 mg IgG/g of membrane. The measured value of equilibrium binding capacity of ≈1,000 mg IgG/g clearly indicates the formation of multiple layers of IgG adsorbed on the fibers by penetration through the grafts. With a hydrodynamic diameter of 100 Å, IgG molecules can easily form several protein layers within the grafts, ultimately leading to remarkable values of equilibrium binding capacity.

The flow performance of the membrane was then characterized by measuring the flow permeability and the $DBC_{10\%}$ at different fluid velocities. The pressure drop per unit length ($\Delta P/L$) was found to increase linearly from 16.9 to 118.7 kPa/cm at 229.2 to 763.9 cm/h (corresponding to RT in the range of 0.1–0.33 min RT, as shown in Fig. S1). The thickness of the membrane adsorber column was approximately 1.25 cm (50 membrane layers). Since the grafted layers can expand and contract in response to changes in pH (charge) and ionic strength, the pressure drop in these types of membranes can vary significantly depending on buffer conditions. These pressure-flow experiments were conducted at pH 5.5 in which the membrane is negatively charged, and at low ionic strength (50 mM acetate buffer), so that the grafted layer should be fully extended, and the pressure drop should be at its

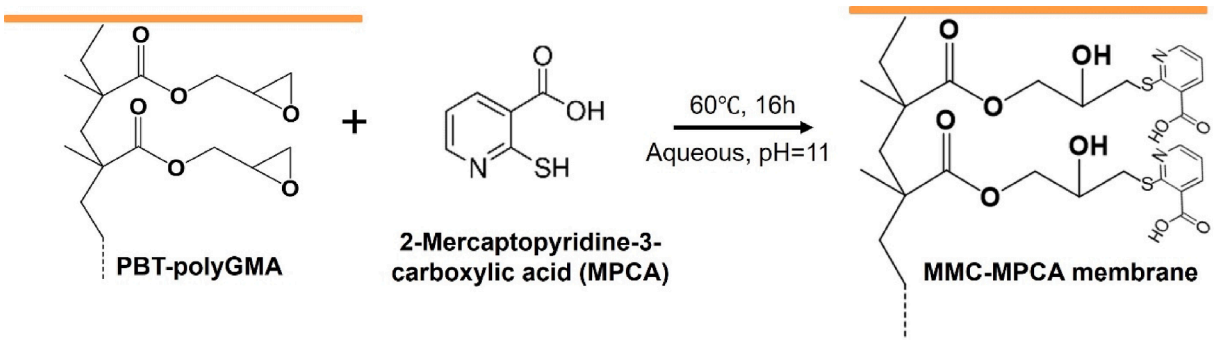


**Fig.1.** Chemical reaction used for coupling MPCA to polyGMA grafted PBT membranes.

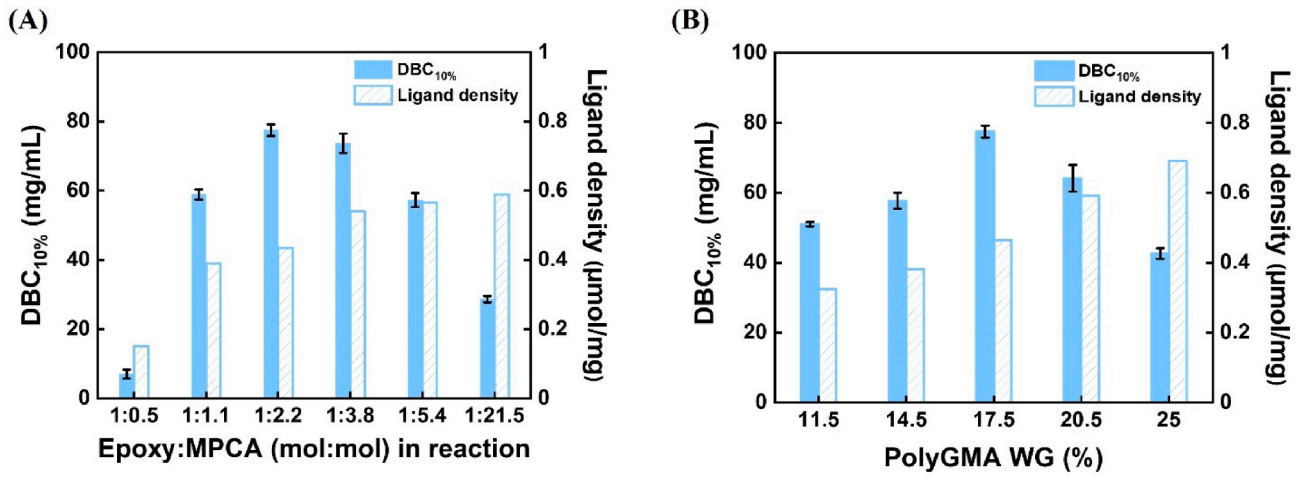


**Fig. 2.** (A) Effect of epoxy/MPCA molar ratio in the ligand coupling reaction solution on $DBC_{10\%}$ of MMC-MPCA membranes at 1.0 min RT with an average 17.5 % WG; (B) Effect of grafted polyGMA %WG on $DBC_{10\%}$ of MMC-MPCA membranes prepared using 1:2.2 epoxy/MPCA molar ratio at 1.0 min RT.

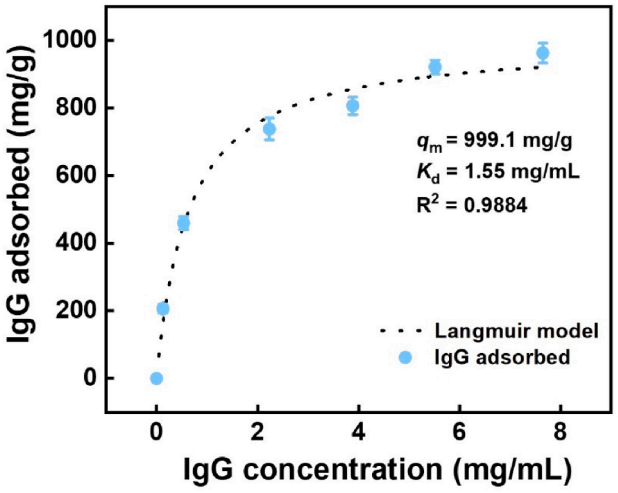


**Fig. 3.** Equilibrium adsorption isotherm of IgG onto MMC-MPCA membrane. Initial IgG solution: 1.0 to 12.5 mg IgG/mL dissolved in pH 5.5 50 mM acetate buffer with added 150 mM NaCl (≈17.5 mS/cm). Experimental data are compared with the fitted data based on the Langmuir model.

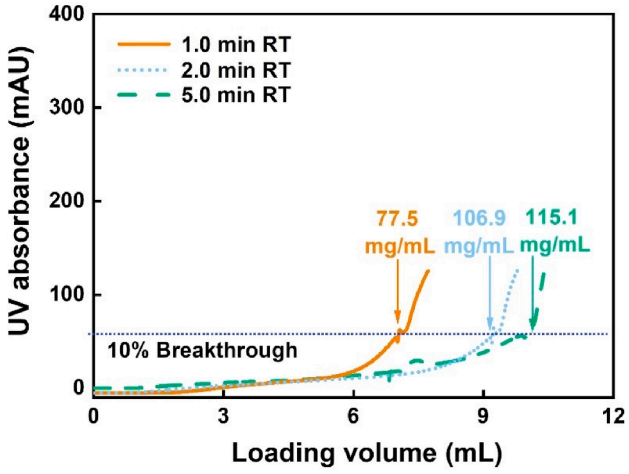


**Fig. 4.** Breakthrough curves at different RTs. Experiments performed by feeding 3.0 mg/mL of IgG on a membrane column of 0.24 mL volume (12 layers, 1.0 cm diameter, ≈0.3 cm membrane bed height).

maximum. The relative permeability of the membrane calculated in these conditions using Eq. (2) was $2.4 \times 10^{-9}$ $cm^2$. The column pressure drops (from 16.9 to 118.7 kPa/cm at 229.2 to 763.9 cm/h) measured in these experiments never went beyond 0.15 MPa (1.5 bars), well within acceptable pressure ranges for flow devices in downstream operations (4–8 bars).

The 10% breakthrough curves obtained in flow experiments with polyclonal IgG at different residence times (RTs) are reported in Fig. 4. The membrane adsorber layer used in these dynamic binding capacity experiments was 0.3 cm thick (12 membrane layers). When increasing the RT from 1.0 to 5.0 min, the corresponding $DBC_{10\%}$ increased from 77.5 mg/mL to 115.1 mg/mL of column. This is a clear indication that there are diffusional effects controlling the adsorption of proteins into the grafted layers. It takes hours for the equilibrium adsorption to occur, and with a RT of 5.0 min the grafted layers are only able to adsorb roughly 37% of their maximum or equilibrium capacity (312.2 mg/mL dry membrane). When the RT is lowered to 1.0 min there is even less time for diffusion through the grafted layers, and the membranes only reach 24.8% of their maximum capacity. Nevertheless, when compared with commercial MMC adsorbents operated under the same conditions (with ≈150 mM NaCl in pH 4.3–6.5 binding buffers), the MMC-MPCA membrane featured significantly higher values of $DBC_{10\%}$ (Table 1) at all values of RTs. We also found that the bound IgG can be completely eluted by 50 mM phosphate buffer at 0.15 M NaCl pH 8.5, which avoided the high concentrations of chaotropic salt (*e.g.*, NaSCN) used in multimodal membranes and resins. This is likely due to a combination of a lower ligand density on the MMC-MPCA membrane (127 mmol/L vs. 340 mmol/L [13]) and the milder hydrophobicity of the pyridine of the ligand. The elution conditions for MMC-MPCA are also milder than the

**Table 1**
Comparison of $DBC_{10\%}$ of multimodal cation exchange adsorbents. The IgG loading solution contained 150 mM NaCl (≈17 mS/cm) at pH 4.3–6.5.

| Adsorbent | RT (min) | IgG $DBC_{10\%}$ (mg/mL) | Elution conditions |
|---|---|---|---|
| Capto™ MMC Impress resin | 4–5 | 50–60 [13] | 1.0 M NaCl at pH 6.0 [37] |
| Nuvia cPrime resin | N/A | 40 [38] | 0.4 M NaCl at pH 7.0 [38] |
| Toyopearl MX-Trp-650M resin | 1 | 48 [39] | 1.0 M NaCl at pH 7.0 [39] |
| 4-Mercaptobenzoic acid cast cellulose membrane | 1 | 38 [13] | 1.0 M NaSCN at pH 8.0 [13] |
| MMC-MPCA membrane (This study) | 1–5 | 77.5–115.1 | 0.15 M NaCl at pH 8.5 |

pH 2.5 elution used for another multimodal membrane with 2-mercaptobenzimidazole as ligand (no cation exchange moiety, 156 mmol/L [23]).

The MMC-MPCA membrane was designed for single use which requires robust reusability in several chromatographic cycles in one campaign before disposal. Accordingly, the stability of the membrane performance was examined by measuring $DBC_{10\%}$ for IgG in five bind-and-elute chromatographic cycles (Section 2.4) at 1.0 min RT. The membrane was cleaned and regenerated with 2.0 M guanidine after elution in each cycle. These experiments generated five chromatograms with identical elution peaks (Fig. 5A) and corresponding values of $DBC_{10\%}$ (Fig. 5B), demonstrating the good reusability of the MMC-MPCA membrane without loss of performance and 2.0 M guanidine is effective for membrane regeneration.

### 3.2. Effects of salt and pH on IgG binding and elution behavior of MMC-MPCA membrane

To elucidate the salt-tolerant properties of the MMC-MPCA membrane, the protein binding ability was evaluated by varying the NaCl concentrations in the binding buffer (pH 5.5) from 0 to 450 mM (Fig. 6A), while maintaining the IgG concentration in the feed at 5.0 mg/mL. At low salt concentration (50 mM) the adsorbed IgG on the membrane increased to 731.5 from 470.1 mg/g with no added salts. This is likely due to strong electrostatic repulsion between charged groups on the membrane at low salt concentration helping to expand the polymer

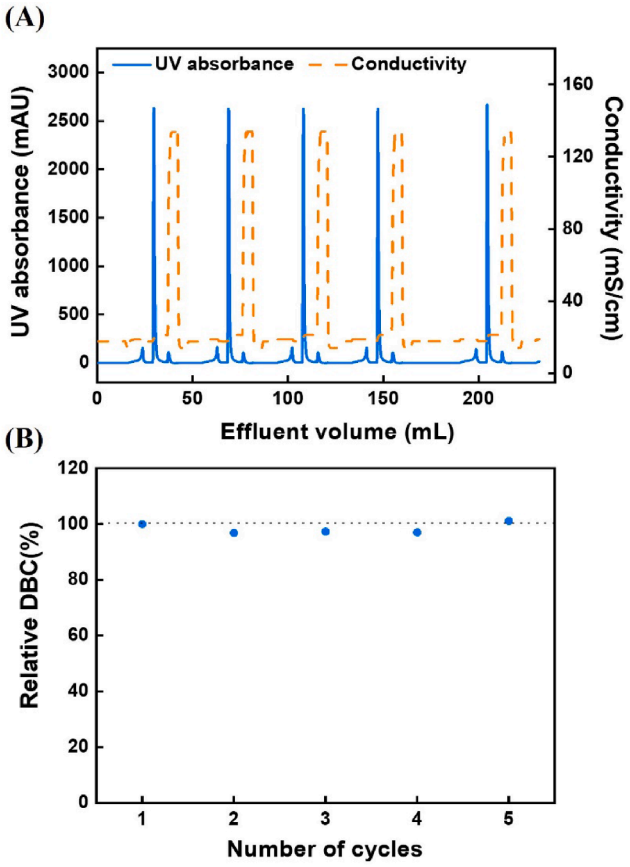


**Fig. 5.** (A) The chromatogram of five consecutive cycles of $DBC_{10\%}$ measurement with 12 layers of MMC-MPCA membrane with 10 mm diameter (0.24 mL membrane volume) at 1.0 min RT (0.24 mL/min flow rate) and (B) relative DBC (ratio of $DBC_{10\%}$ obtained in subsequent cycle to the one in the first cycle). The membranes were regenerated with 7.2 mL 2.0 M guanidine-HCl after each cycle followed by membrane re-equilibration with 12 mL binding buffer before the next cycle.

grafts. One the other hand, the added salt enhanced the hydrophobic interaction, which also contributed to the higher binding capacity compared to that without added NaCl. This phenomenon differs from the behavior reported for other salt tolerant resins and membranes, where the highest protein binding occurs in solutions without any added salts [40,41]. The binding capacity of the MMC-MPCA membrane remained essentially constant in the salt concentration range of 50–150 mM, and finally dropped in the range of 300–450 mM, due to a strong charge screening effect between the ligand and IgG, which was unable to be offset by the increased hydrophobic interaction. The high binding capacities in the range of 50–150 mM make the MMC-MPCA membrane ideal adsorbents for product capture directly from unconditioned bioreactor harvests. As shown in Fig. 6B, divalent cation and anion salts ($MgCl_2$ and $Na_2SO_4$) have a stronger impact on protein binding to the MMC-MPCA membrane than monovalent ions (NaCl) at the same concentration. This is expected as the ionic strength increases with the valency of the ion at a given concentration. As a kosmotropic salt, NaCitrate enhanced hydrophobic protein–ligand interactions, thus affording values of IgG adsorption close to those obtained in the NaCl-supplemented buffer. A similar performance was also observed by Wang *et al.* in a study of a multimodal CEX membrane where the IgG binding capacities in the range from 0 to 1.0 M NaCitrate were almost identical [42]. There was little change in binding capacity with $Na_2SO_4$ as the concentration went from 50 to 150 mM, but there was more than a 50% drop when the concentration of $MgCl_2$ increased from 50 to 150 mM. These results are likely to vary from protein to protein and from salt type to salt type, but the observations offer consistent proof of salt tolerance over a broad range of salt concentrations.

Changes in pH can impact the ionization of the ligand and the protein surface, resulting in a wide variation in binding behavior [43,44]. Accordingly, the influence of pH from 4.5 to 7.0 on IgG (average pI ≈ 8.2 [28]) binding to MMC-MPCA membrane was studied. Fig. 7 shows that the IgG adsorption on the membrane increased from 83.6 mg/g at pH 4.5 to 131.0 mg/g at pH 5.0. It reached the highest value at pH 5.5 (754.6 mg/g) then linearly decreased as the pH reached 7.0 (180.9 mg/g). The $pK_a$ of the MPCA ligand is 3.0–4.5, as determined by zeta potential measurement at pH 2.5–11.0 (data not shown), consistent with the *pKa* of carboxyl groups. The lower protein adsorption at pH 4.5 can therefore be ascribed to the insufficient negative charge on the ligand, despite the strong cationic character of IgG at low pH. Increasing negative charge of the ligand from pH 5.0 to 5.5 led to more proteins being adsorbed. On the other hand, as the cationic character of IgG, and thus the binding strength, subsides from pH 5.5 to 7.0, IgG adsorption decreases.

To obtain high protein recovery (mass ratio of the eluted IgG to the bound IgG), the elution efficiency of buffers with different pH and salt concentrations was investigated. As shown in Fig. 8, the elution efficiency of pH 5.5 buffer reached a plateau of 86% at NaCl concentration higher than 1.5 M. This implies that the dominant binding force for IgG on MPCA is electrostatic attraction. This is also evidenced by the poorer elution performance of buffers formulated with urea, ethylene glycol, and arginine (Fig. S2), whose chaotropic character is meant to disrupt hydrophobic interactions, hydrogen bonding, and electrostatic interactions [45,46]. Fig. 8 also shows that the recovery of IgG at pH 8.0 does not reach 100% unless the elution buffer includes high salt concentrations (150 mM NaCl). Conversely, at pH 8.5 and 9.0, recoveries close to 100% are reached with lower salt concentrations of 0.5 M and 0.15 M NaCl, respectively. A possible reason for the better elution performance is the decreased electrostatic attraction between IgG and ligand at pH greater than 8.0 that is close to the average pI of polyclonal IgG.

### 3.3. Capture of a mAb from cell culture harvest using MMC-MCPA membrane

Mixed mode chromatography is a promising alternative to Protein A for direct capture of mAbs from cell culture harvest, owing to its salt

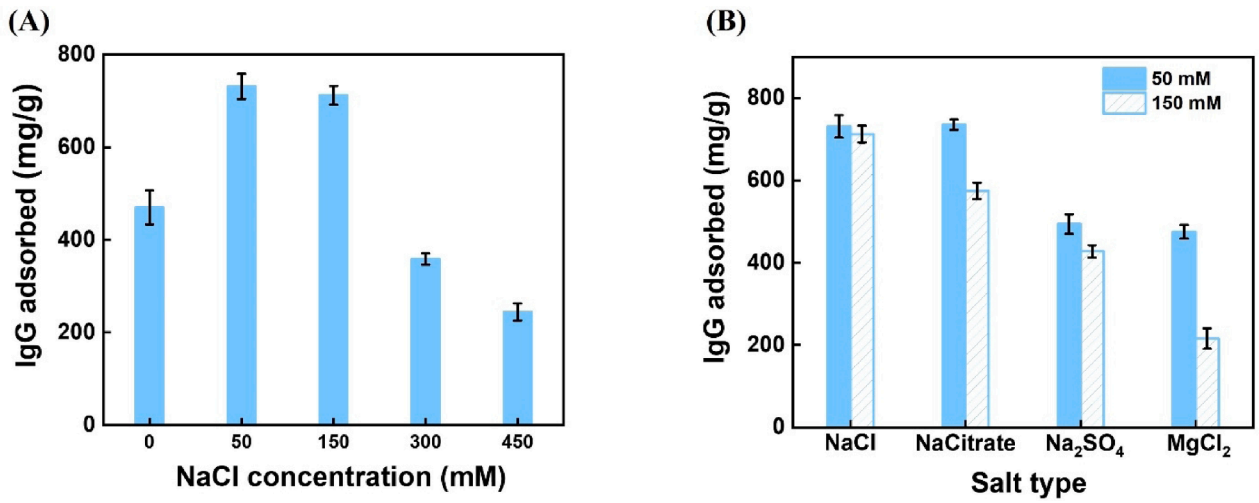


**Fig. 6.** Effect of different NaCl concentrations (A) and effect of different salt types (B) on IgG adsorption to MMC-MCPA membrane with an initial IgG concentration of 5 mg/mL in the 50 mM acetate buffer pH 5.5 with added salts.

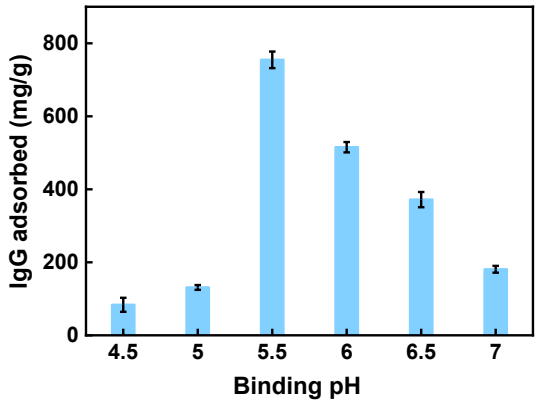


**Fig. 7.** Effect of pH on IgG adsorption on MMC-MPCA membrane: NaCl concentration in 50 mM Na acetate buffer, pH 5.5, adjusted with 1.0 M NaOH or 1.0 M HCl. The initial IgG concentration was 5.0 mg/mL.

tolerance, higher capacity, and lower cost [9,14]. Capto MMC and MX-Trp-650M are two commonly used multimodal cation exchange resins that have gained much attention owing to their good binding capacity and robust separation performance [47,48]. The structures of the ligands on these resins are shown, together with the structure of MPCA, in Fig. 9. The salt tolerant behavior of Capto MMC and MX-Trp-650M is rooted in their hydrophobic phenyl and indole groups, respectively. The combination of electrostatic, thiophilic, hydrophobic and hydrogen bonding interactions of these ligands enable both resins to capture mAbs without the need to adjust the conductivity of the culture harvest. The mAb capture experiments described here were conducted at pH ranges between 4.5 and 5.5, at which the mAb was positively charged (pI ≈ 7.6) and adsorbed efficiently on the negatively charged carboxyl moiety of both ligands. With the pKa of carboxyl groups typically ranging between 3.0 and 4.5 [49], these multimodal ligands operate ideally at pH above 4.5 if the pI of the protein is greater than 4.5. As described above, the MMC-MPCA ligand containing a carboxyl group and a pyridine ring (less hydrophobic than the phenyl and indole), exhibited a high protein binding capacity for polyclonal IgG, and the question remained as to how it would function in capture a monoclonal antibody in a CHO cell culture supernatant.

The capture performance of the MMC-MPCA membrane was therefore evaluated in comparison to that of Capto MMC, MX-Trp-650M resins, as well as a Protein A affinity resin (AF-rProtein A HC-650F) in terms of mAb binding capacity and impurity clearance. Before loading the mAb solution to the multimodal CEX adsorbents, the cell culture fluid (≈11 mS/cm) was adjusted to pH 5.5 for the MMC-MPCA membrane and Capto MMC and to pH 4.5 for MX-Trp-650M since its binding

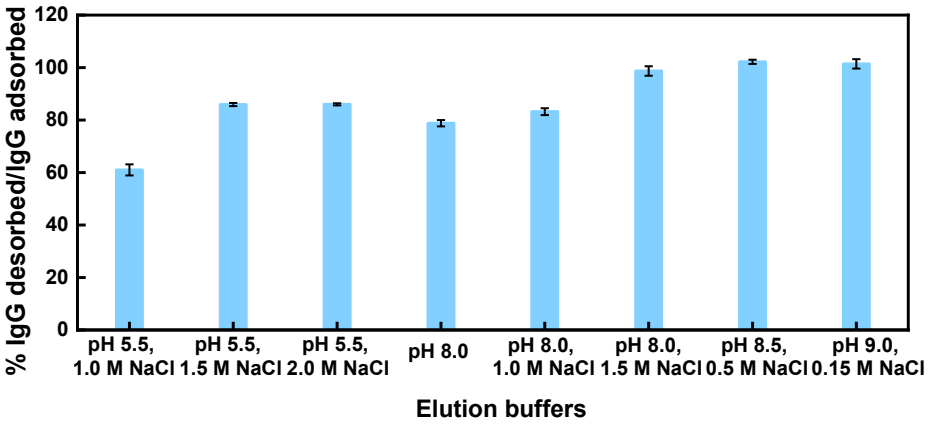


**Fig. 8.** %IgG desorption from MMC-MCPA membrane with different elution buffers. Before elution, the IgG was adsorbed by MMC-MCPA membrane with an initial IgG concentration of 5 mg/mL in a 50 mM acetate pH 5.5 with 0.15 M NaCl. The pH was adjusted by adding 1.0 M NaOH, or 1.0 M HCl and the conductivity was adjusted by adding additional NaCl.

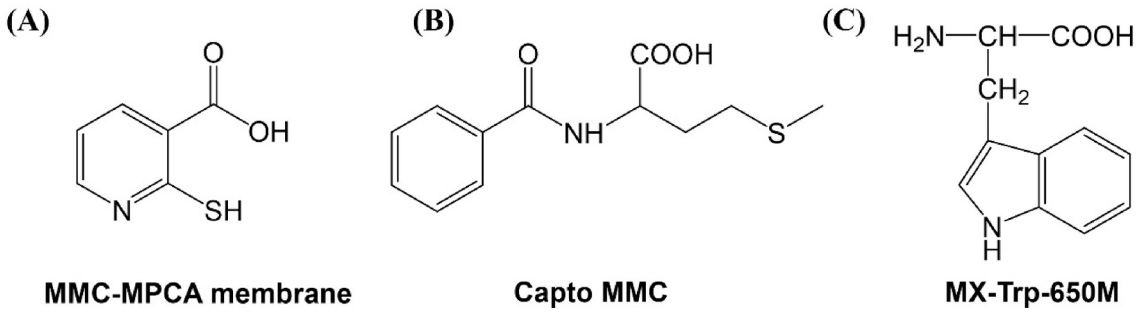


**Fig. 9.** Ligand structures on MMC-MPCA membrane (A), Capto MMC (B) and MX-Trp-650M (C).

capacity was very low at pH 5.5 (6.4 mg/mL, Fig. S3); conversely, the supernatant was loaded without any adjustment on the Protein A affinity column. In all separations, the sample solution was injected at 5.0 min RT. As shown in the chromatograms reported in Fig. 10, the salt tolerant CEX media were first equilibrated with pH 5.5 (or pH 4.5) buffer. After sample loading, the three media were washed with equilibration buffer, and protein elution was finally conducted at pH 9.0 with 0.15 M NaCl. The equilibration, washing, and elution steps for the MMC-MPCA membrane were processed at 0.5 min RT, while for the resins a 5.0 min RT was used. As shown in Table 2, the MMC-MPCA membrane obtained a higher mass of the eluted mAb per mL of column volume than the resins. The MMC-MPCA membrane and Capto MMC resin achieved similar HCP log removal values, which were better than the HCP removal by the MX-Trp-650M resin. The MMC-MPCA membrane also reduced the aggregate levels from 5.4% in the feed solution to 2.5% in the eluate. This removal performance is slightly better than those of the resins since the aggregates tend to be more hydrophobic than the mAb monomer [50] and are likely to adsorb more strongly to hydrophobic ligands. An additional wash with 0.1 M arginine solution after sample loading was used to optimize the IgG isolation using the MMC-MPCA membrane, as shown in Fig. 10D. With an additional 0.1 M arginine wash, both the HCPs and aggregate clearance were improved. Arginine is known to weaken hydrophobic interactions between HCPs and mAbs products bound to resins [51]. As anticipated, the Protein A affinity column showed a better HCPs removal performance (chromatogram shown in Fig. 10**E**), however there were more aggregates (11.9%) likely generated by the pH 3.0 elution buffer (the collected eluate was neutralized immediately after elution). Collectively, these results portray the CEX-MPCA membrane as a viable alternative for capture of mAbs that are sensitive to low pH.

### *3.4. mAb polishing following protein A chromatography using MMC-MPCA in bind-and-elute mode*

Multimodal cation exchange chromatography has been introduced into mAb purification as an effective polishing step after the affinity-based capture step [11,52]. Zhang *et al.* [5] and Wolfe *et al.* [46] exploited the unique selectivity of Capto MMC resin, and obtained good aggregate and HCP removal for mAb polishing in bind-and-elute mode with model-based process development and optimization of modulators in the mobile phase. Tang *et al.* [53] and Zhang *et al.* [54] processed a Protein A eluate by Capto MMC ImpRes and Capto MMC resins with good aggregate removal at 5.0 min RT.

We anticipated that the MMC-MPCA membrane could be used to process the Protein A eluate not only without the need to reduce the conductivity, but also by operating at shorter residence times. Accordingly, MMC-MPCA membranes packed in a 0.25 mL column were loaded with 2.0 mL of the Protein A eluate (6.1 mg mAb/mL, 1319.7 ppm HCPs, 11.9% aggregates, ≈19 mS/cm, pH 5.5, Table 2) using a RT of 2 min for sample loading and 0.5 min for the washing and elution steps. The relevant chromatograms are displayed in Fig. 11 and the results are listed in Table 3. A high mAb recovery of 95% was obtained (calculated DBC was 52.0 mg/mL). By comparing the DBC of ≈53 mg/mL (in Table 2) obtained in the capture step where feed solution was CHO supernatant (2.2 mg/mL mAb) at the same RT, it indicates the binding capacity of CEX-MPCA membrane is quite stable and barely affected by impurities and different concentrations of mAb (2.2–6.1 mg/mL) in the feed. The aggregate content decreased to 6.7% and the residual HCP level was 62.4 ppm. The HCPs and mAb aggregates content in the elution fraction were further reduced by a 0.1 M arginine wash step following protein loading (Fig. 11 and Table 3). When employing a pH gradient elution (pH 7.6, 8.3 9.0) and collecting mAb at pH 7.6 (Fig. 11**C**), a lower titer of residual HCPs of 48.7 ppm was obtained, corresponding to an LRV of 1.43. In the SDS-PAGE analysis with silver staining shown in Fig. S4 the removal of HCP was not easily apparent. According to the Protein G analysis shown in Fig. S5, the purity of the eluted mAb was close to 100% with no visible impurity peak in the chromatogram, showing an improvement from the 98.0% purity of the eluate from Protein A column. The aggregate content was further reduced to 4.4%. The size exclusion HPLC results in Fig. S6 show that the aggregates were effectively removed by the pH 7.6 elution, especially those with higher molecular weight (10–12 min retention time) that were present in the pH 9.0 eluate, since they are generally more positively charged compared to the monomeric mAb [5,55]. Overall, according to the size exclusion HPLC chromatograms in Fig. S7, the Protein A column removed a large fraction of the impurities including small substances, HCPs (20–40 min retention time), larger aggregates and DNA (10–12 min retention time) from the supernatant. The MMC-MPCA membrane further cleared larger aggregates (much smaller peak at 12 min retention time) and HCPs at exhibiting higher retention times.

### *3.5. Proteomic analysis*

To further assess the effectiveness of the MMC-MPCA membrane in HCP removal and evaluate the overall clearance performance of the combination of Protein A resin and the membrane in a bind-and-elute mode, we analyzed in-process samples using a proteomics approach (described in Section 2.6). Fig. S8 shows distribution plots of the number of HCPs encountered at each stage and their distribution of isoelectric points; cell culture fluid (CCF) that was loaded into the Protein A column; the pH adjusted and filtered Protein A eluate that was applied to the MPCA membrane; and finally, the membrane eluate at pH 7.6 in a pH gradient elution shown in the chromatogram Fig. 11C. The profiles of pI distribution (4–12) of HCPs in the load CCF, in the Protein A eluate, and in the membrane eluate, are similar while the overall number of HCPs identified decreased after Protein A column and was furthered reduced by the membrane. We detected 1990 HCPs, either secreted or released by CHO cells, in the load sample (≈300,000 ppm HCPs) applied to Protein A column. A list of 32 of these host proteins was then curated and tracked throughout purification processes, as they have previously been identified and reported as high-risk and highly prevalent in CHO

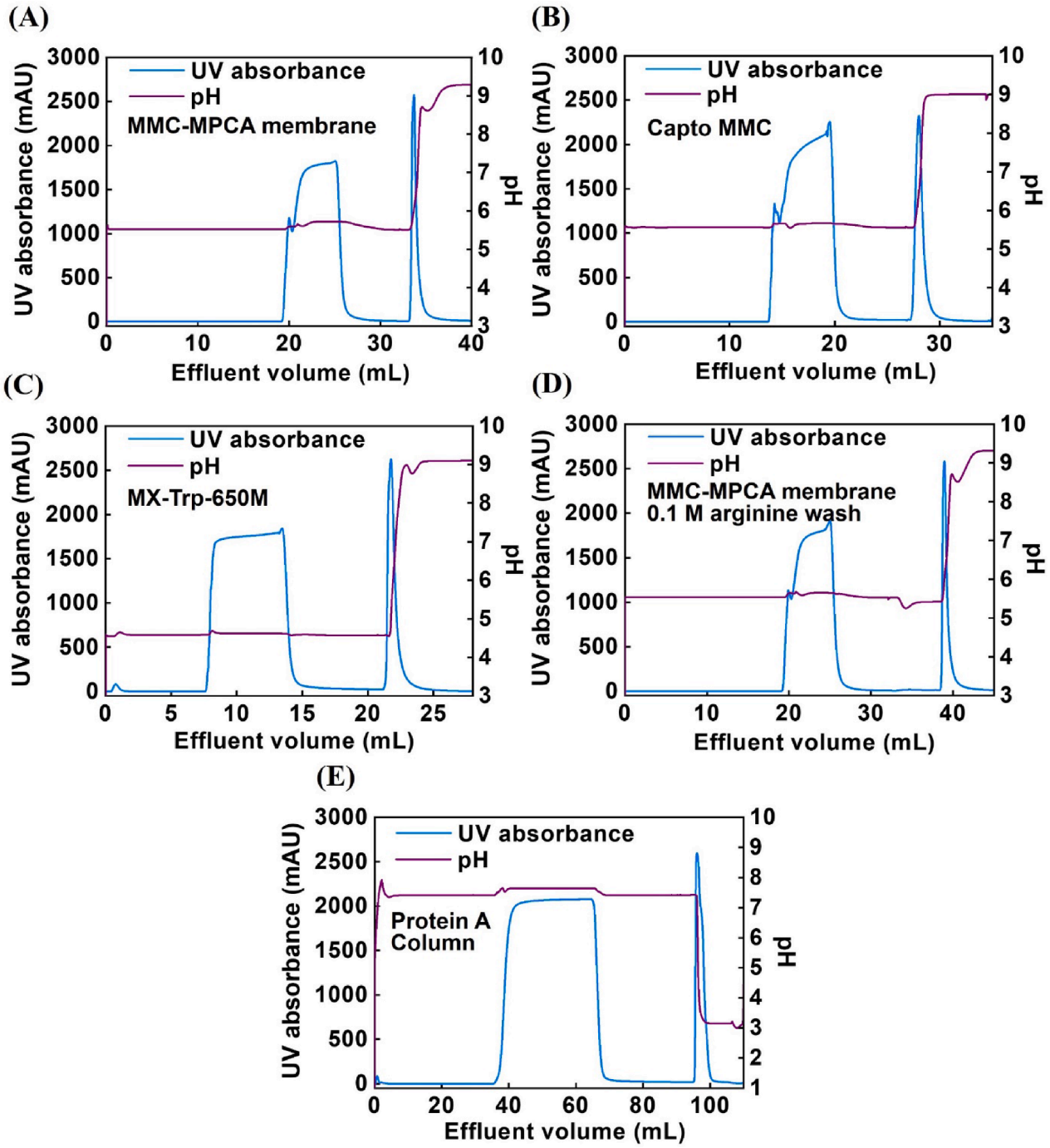


**Fig. 10.** mAb capture by MMC-MPCA membrane (A), Capto MMC (B), MX-Trp-650M (C), MMC-MPCA membrane with additional 0.1 M arginine in wash step following sample loading (D), and AF-rProtein A HC-650F (E).

**Table 2**
Results of mAb capture by MMC-MPCA membrane, Capto MMC, MX-Trp-650M and AF-rProtein A.

| Separation media | pH | Additional wash | DBC[1] (mg/mL) | Recovery[2] (%) | HCP[3] (LRV) | Aggregates (%) |
|---|---|---|---|---|---|---|
| MMC-MPCA membrane | 5.5 | N/A | 52.8 | 96.4 | 0.48 | 2.5 |
| Capto™ MMC | 5.5 | N/A | 35.1 | 63.9 | 0.46 | 3.3 |
| Toyopearl MX-Trp-650M | 4.5 | N/A | 46.4 | 93.3 | 0.23 | 3.2 |
| MMC-MPCA membrane | 5.5 | 0.1 M Arginine | 53.0 | 96.8 | 0.67 | 2.0 |
| AF-rProtein A | 7.4 | N/A | 32.1 | 93.0 | 2.3 | 11.9 |

[1] DBC calculated as the mass of the eluted mAb divided by the volume of membrane or resin.
[2] Recovery calculated as the mass ratio of the eluted mAb to the mAb applied in the loading solution.
[3] 300,000 ppm (ng HCP/mg of mAb) HCP in the feed solution (CHO supernatant).

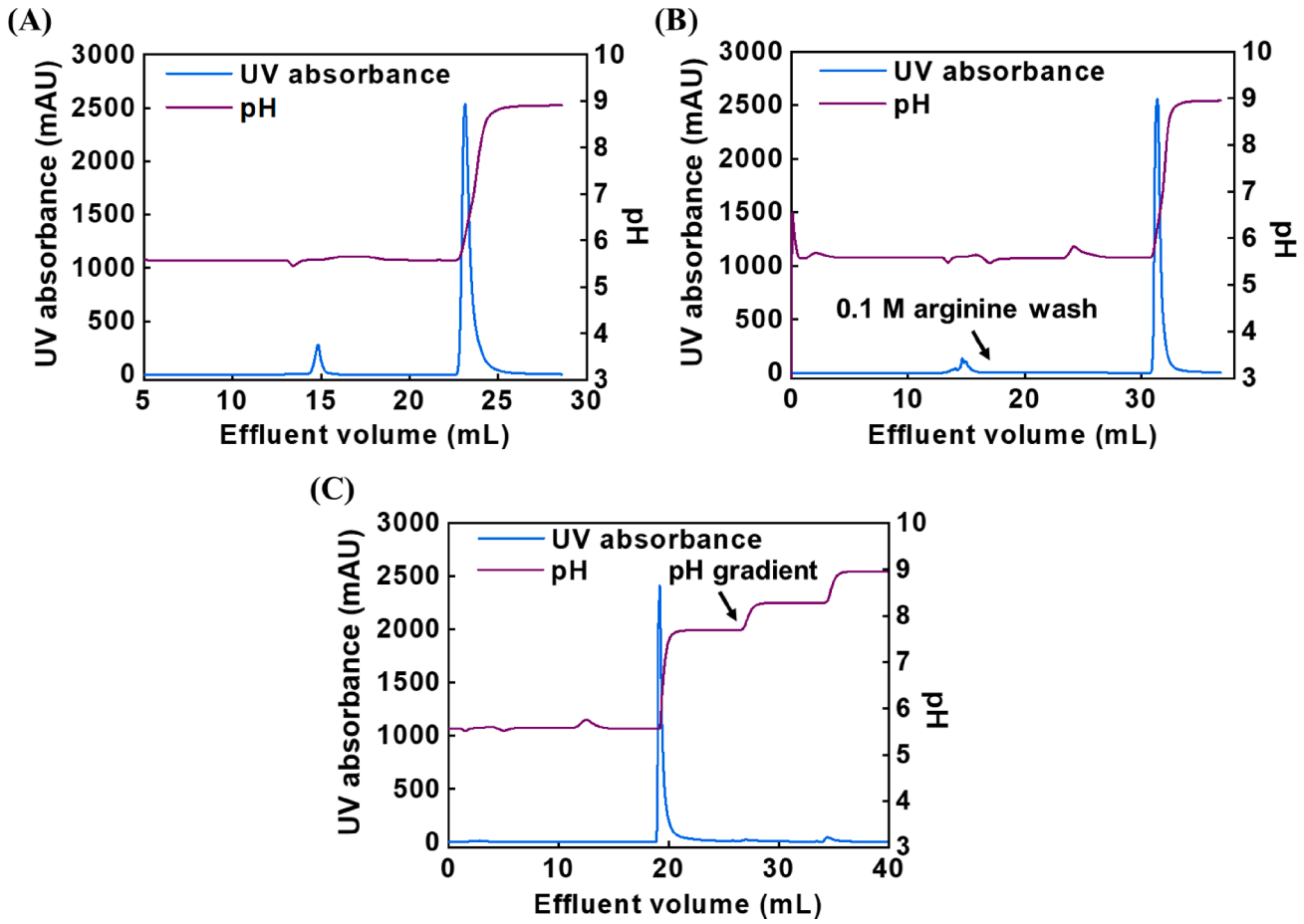


**Fig. 11.** mAb polishing by MMC-MPCA membrane with different separation conditions. No process optimization (A), additional 0.1 M arginine in membrane wash (B), additional 0.1 M arginine in membrane wash and pH gradient elution (pH 7.6, 8.3, 9.0) (C). Membrane volume: 0.24 mL; sample loading volume: 2.0 mL; RT: 2.0 min.

**Table 3**
Results of mAb polishing by MMC-MPCA membrane with different separation conditions.

| Separation optimization | Loading volume (mL) | DBC (mg/mL) | Recovery (%) | HCP (LRV) | HCP content (ppm) | Aggregates (%) |
|---|---|---|---|---|---|---|
| Standard conditions | 2.0 | 52.0 | 95.1 | 1.32 | 62.4 | 6.7 |
| 0.1 M arginine wash | 2.0 | 55.9 | 98.2 | 1.37 | 56.6 | 5.1 |
| 0.1 M arginine wash and pH gradient elution | 2.0 | 50.4 | 92.1 | 1.43 | 48.7 | 4.4 |

bioprocesses [31,56] in Table 4. Furthermore, a risk class has been assigned to these proteins based on the nature of risks they have been associated with, i.e., (1) HCPs that co-elute with mAb products and/or degrade the mAb, and (2) HCPs identified as immunogenic that pose risk to patient safety. Individual protein abundances obtained using proteomics analyses were utilized to calculate the relative abundance of each species for perspective analyses and the values were utilized to conduct statistical significance analyses to determine reduction in HCP levels.

The protein A eluate showed a good reduction in the total number of HCPs (645 species, remaining corresponding to measured HCP concentration of 1319.7 ppm) whose cumulative abundance was found to make up for <5% of the total sample abundance, compared to those observed in the load sample (963 species). As seen in Table 4, further high-risk HCP tracking showed that the protein A step was ineffective in removing 22 of total 32 high-risk HCPs, with just 31.25% of these species significantly reduced, highlighting the need for additional polishing steps. Implementation of the MMC-MPCA membrane (48.7 ppm residue HCPs after membrane separation) was successful in further removal of 15 high-risk HCPs and a total, numeric 62.5% of these species through the combination of protein A and MMC-MPCA membrane, demonstrating the excellent clearance for high-risk HCPs by the novel membrane. Retained high-risk HCPs mostly consisted of Cathepsin B, BiP precursor, Matrix Metalloproteinase-19, Peptidyl-prolyl cis–trans isomerases, legumain, and PLBL-2. These proteins could 'hitchhike' with mAbs during separation or interact with the ligand hence co-eluting with it. Further investigation into this phenomenon is beyond the scope of this study. On the other hand, these proteins can alternatively be depleted using LigaGuard™, a peptide-based technology developed and reported by our group [30,57]. This work therefore can be extended to study mAb purification by the combination of inexpensive nonwovens and peptide-based adsorbents in the future.

## 4. Conclusions

In this study, a new MMC membrane was developed by attaching MPCA to the polyGMA grafted PBT nonwoven fabric. It exhibited a high $DBC_{10\%}$ of 77.5–115.1 mg IgG/mL (1.0–5.0 min RT) which is 2-to-3-fold higher than those of commercial MMC adsorbents, a good flow permeability of $2.4 \times 10^{-9}$ $cm^2$ that makes the pressure drop (<1.5 bar at 0.1–0.33 min RT) well below acceptable pressure ranges for flow devices

**Table 4**
Profile of high-risk HCPs cleared and retained in eluates. These HCPs have been categorized based on their risk class: (1) indicates HCPs observed to affect drug stability, formulation, or those reported to co-elute and (2) indicates HCPs involved in eliciting unwanted immune responses. The color gradient indicates significantly removed high-risk HCP (green, $p < 0.05$) to those not removed (red, $p \gg 0.05$).

| Accession | High-risk HCPs | Risk Category | HR-HCP removal in Protein-A eluate compared to presence in Load Sample | HR-HCP removal in MMC-MPCA eluate compared to Protein-A eluate |
|---|---|---|---|---|
| XP_027270017.1 | 60S acidic ribosomal protein P0 isoform X1 | 1 | 0.80 | 0.05 |
| XP_027257976.1 | 60S ribosomal protein L17 | 1 | 0.06 | 0.00 |
| XP_027246095.1 | 60S ribosomal protein L5 | 1 | 0.33 | 0.00 |
| XP_027251387.1 | 60S ribosomal protein L9 | 1 | 0.74 | 0.00 |
| XP_027254100.1 | alpha-enolase isoform X2 | 1 | 0.38 | 0.02 |
| XP_027247784.1 | annexin A5 | 2 | 0.00 | 0.00 |
| XP_027246161.1 | cathepsin B | 1 | 0.00 | 0.98 |
| XP_027264700.1 | cathepsin D | 1 | 0.00 | 0.00 |
| XP_027265420.1 | cathepsin L1 | 1 | 0.13 | 0.12 |
| XP_027275654.1 | cathepsin Z | 1 | 0.00 | 0.05 |
| XP_027246102.1 | clusterin | 2 | 0.85 | 0.00 |
| NP_001233668.1 | endoplasmic reticulum chaperone BiP precursor | 1 | 0.13 | 0.67 |
| XP_027243453.1 | enolase-phosphatase E1 isoform X1 | 1 | 0.65 | 0.00 |
| XP_027266901.1 | glutathione S-transferase A4 | 2 | 0.71 | 0.00 |
| NP_001233649.1 | heat shock protein 105 kDa | 1 | 0.01 | 0.53 |
| NP_001233750.1 | heat shock protein HSP 90-alpha | 1 | 0.73 | 0.00 |
| XP_027265307.1 | histone H2A type 1-H isoform X1 | 2 | 0.39 | 0.00 |
| XP_027265357.1 | histone H3 isoform X2 | 2 | 0.62 | 0.23 |
| XP_027274961.1 | legumain | 1 | 0.00 | 0.60 |
| XP_027244681.1 | lipoprotein lipase isoform X1 | 1 | 0.66 | 0.00 |
| XP_027247933.1 | matrix metalloproteinase-19 | 1 | 0.73 | 0.98 |
| XP_027265239.1 | nidogen-1 isoform X3 | 1 | 0.10 | 0.01 |
| XP_027267107.1 | peptidyl-prolyl cis-trans isomerase B | 1 | 0.00 | 0.94 |
| XP_027285515.1 | peptidyl-prolyl cis-trans isomerase FKBP9 | 1 | 0.71 | 0.62 |
| XP_027253977.1 | procollagen-lysine,2-oxoglutarate 5-dioxygenase 1 isoform X3 | 2 | 0.40 | 0.00 |
| XP_027249169.1 | protein S100-A6 isoform X1 | 2 | 0.00 | 0.00 |
| XP_027269956.1 | putative phospholipase B-like 2 | 2 | 0.15 | 0.39 |
| XP_027270674.1 | pyruvate kinase PKM isoform X2 | 2 | 0.96 | 0.03 |
| XP_027260200.1 | serine protease HTRA1 isoform X2 | 1 | 0.65 | 0.08 |
| XP_027283254.1 | SPARC isoform X3 | 1 | 0.13 | 0.08 |
| XP_027286179.1 | transforming growth factor beta-1 proprotein isoform X2 | 2 | 0.48 | 0.00 |
| XP_027261047.1 | vimentin | 1 | 0.00 | 0.05 |

(4–8 bars), as well as a robust reusability without loss of $DBC_{10\%}$ for IgG in five repeated bind-and-elute chromatographic cycles. These features make the membrane a promising alternative to resins for fast and efficient protein purification. The static binding capacity of the membrane was found to remain high and stable around 700 mg IgG/g at 50–150 mM NaCl in pH 5.5 acetate buffer. This excellent salt tolerance can enable the membrane to process biological solutions without buffer exchange or dilution, which are often required in conventional ion exchange chromatography, reducing material cost and time. The elution condition (50 mM phosphate buffer pH 8.5 at 0.15 M NaCl) is much milder compared to high concentrations of chaotropic salts and low-pH buffers used for other reported multimodal membranes. In real applications, the MMC-MPCA membrane achieved a higher mAb binding capacity and better performance for HCPs and aggregates removal than commercial multimodal CEX resins in the mAb capture step and fewer aggregates in the eluate when compared to Protein A resin (while the Protein A resin had a better HCPs removal with a higher selectivity). In addition, a fast polishing of Protein A eluate reduced the HCP level to 48.7 ppm with a LRV of 1.43 - well below the common requirement of < 100 ppm for mAb products. Proteomic analysis confirmed that the MMC-MPCA membrane further removed 15 high-risk HCPs compared to those retained in the eluate from the Protein A column. We demonstrated that the MMC-MPCA membrane could provide an effective alternative to resin columns and other currently available membranes for improving production efficiency in mAb biomanufacturing. Future efforts aim at establishing large productivity and low-cost Protein A-free mAb purification by integration of this new single-use nonwoven membrane adsorber with peptide-based resins for HCP depletion [30,57], developing continuous or hybrid mAb purification processes, as well as broadening its applications for purification of pH-sensitive mAbs, other non-mAb proteins, and viral vectors from various culture fluids.

## Declaration of Competing Interest

The authors declare that they have no known competing financial interests or personal relationships that could have appeared to influence

the work reported in this paper.

## Data availability

Data will be made available on request.

## Acknowledgments

This research was funded by the William R. Kenan, Jr. Institute for Engineering, Technology and Science at NC State University and the Novo Nordisk Foundation (Grant # NNF19SA0035474). We gratefully acknowledge the support of the staff of the Golden LEAF Biomanufacturing Training and Education Center (BTEC) and the Molecular Education, Technology, and Research Innovation Center (METRIC) at NC State University.

## Appendix A. Supplementary material

Supplementary data to this article can be found online at https://doi.org/10.1016/j.seppur.2023.123920.

## References

[1] R.M. Lu, Y.C. Hwang, I.J. Liu, C.C. Lee, H.Z. Tsai, H.J. Li, H.C. Wu, Development of therapeutic antibodies for the treatment of diseases, J. Biomed. Sci. 27 (2020) 30.
[2] J. Winderl, E. Neumann, J. Hubbuch, Exploration of fiber-based cation exchange adsorbents for the removal of monoclonal antibody aggregates, J. Chromatogr. A 1654 (2021) 12.
[3] S. Vogg, F. Pfeifer, N. Ulmer, M. Morbidelli, Process intensification by frontal chromatography: performance comparison of resin and membrane adsorber for monovalent antibody aggregate removal, Biotechnol. Bioeng. 117 (2020) 662–672.
[4] N. Mustafaoglu, T. Kiziltepe, B. Bilgicer, Antibody purification via affinity membrane chromatography method utilizing nucleotide binding site targeting with a small molecule, Analyst 141 (2016) 6571–6582.
[5] L. Zhang, S. Parasnavis, Z.J. Li, J. Chen, S. Cramer, Mechanistic modeling based process development for monoclonal antibody monomer-aggregate separations in multimodal cation exchange chromatography, J. Chromatogr. A 1602 (2019) 317–325.
[6] K. Behere, S. Yoon, Chromatography bioseparation technologies and in-silico modelings for continuous production of biotherapeutics, J. Chromatogr. A 1627 (2020) 11.
[7] V. Halan, S. Maity, R. Bhambure, A.S. Rathore, Multimodal chromatography for purification of biotherapeuties - a review, Curr. Protein Pept. Sci. 20 (2019) 4–13.
[8] S. Maria, G. Joucla, B. Garbay, W. Dieryck, A.M. Lomenech, X. Santarelli, C. Cabanne, Purification process of recombinant monoclonal antibodies with mixed mode chromatography, J. Chromatogr. A 1393 (2015) 57–64.
[9] K.A. Kaleas, M. Tripodi, S. Revelli, V. Sharma, S.A. Pizarro, Evaluation of a multimodal resin for selective capture of CHO-derived monoclonal antibodies directly from harvested cell culture fluid, J. Chromatogr. B 969 (2014) 256–263.
[10] I.F. Pinto, M.R. Aires-Barros, A.M. Azevedo, Multimodal chromatography: debottlenecking the downstream processing of monoclonal antibodies, Pharm. Bioprocess. 3 (2015) 263–279.
[11] E. O'Connor, M. Aspelund, F. Bartnik, M. Berge, K. Coughlin, M. Kambarami, D. Spencer, H.M. Yan, W. Wang, Monoclonal antibody fragment removal mediated by mixed mode resins, J. Chromatogr. A 1499 (2017) 65–77.
[12] J. Osuofa, D. Henn, J.X. Zhou, A. Forsyth, S.M. Husson, High-capacity multimodal anion-exchange membranes for polishing of therapeutic proteins, Biotechnol. Progr. 37 (2021) 11.
[13] J. Wang, E.W. Jenkins, J.R. Robinson, A. Wilson, S.M. Husson, A new multimodal membrane adsorber for monoclonal antibody purifications, J. Membrane. Sci. 492 (2015) 137–146.
[14] M. Dileo, A. Ley, A.E. Nixon, J. Chen, Choices of capture chromatography technology in antibody manufacturing processes, J. Chromatogr. B 1068 (2017) 136–148.
[15] J. Wang, J.X. Zhou, Y.K. Gowtham, S.W. Harcum, S.M. Husson, Antibody purification from CHO cell supernatant using new multimodal membranes, Biotechnol. Progr. 33 (2017) 658–665.
[16] L.E. Crowell, C. Goodwine, C.S. Holt, L. Rocha, C. Vega, S.A. Rodriguez, N. C. Dalvie, M.K. Tracey, M. Puntel, A. Wigdorovitz, V. Parreno, K.R. Love, S. M. Cramer, J.C. Love, Development of a platform process for the production and purification of single-domain antibodies, Biotechnol. Bioeng. 118 (2021) 3348–3358.
[17] M. Toueille, A. Uzel, J.F. Depoisier, R. Gantier, Designing new monoclonal antibody purification processes using mixed-mode chromatography sorbents, J. Chromatogr. B 879 (2011) 836–843.
[18] L.I. Sakhnini, A.K. Pedersen, I.R. Leon, P.J. Greisen, J.J. Hansen, M.B. Vester-Christensen, L. Bulow, M.B. Dainiak, Optimizing selectivity of anion hydrophobic multimodal chromatography for purification of a single-chain variable fragment, Eng. Life Sci. 19 (2019) 490–501.
[19] J.C. Cordova, S. Sun, J. Bos, S. Thirumalairajan, S. Ghone, M. Hirai, R.A. Busse, J.S. V. der Hardt, I. Schwartz, J.Y. Zhou, Development of a single-step antibody-drug conjugate purification process with membrane chromatography, J. Clin. Med. 10 (2021) 14.
[20] C. Boi, S. Dimartino, Advances in membrane chromatography for the capture step of monoclonal antibodies, Curr. Org. Chem. 21 (2017) 1753–1759.
[21] R. Ghosh, G.Q. Chen, R. Roshankhah, U. Umatheva, P. Gatt, A z(2) laterally-fed membrane chromatography device for fast high-resolution purification of biopharmaceuticals, J. Chromatogr. A 1629 (2020) 10.
[22] Z.Z. Liu, S.R. Wickramasinghe, X.H. Qian, Membrane chromatography for protein purifications from ligand design to functionalization, Sep. Sci. Technol. 52 (2017) 299–319.
[23] N. Ma, D.X. Yao, H. Yang, J. Yin, H. Wang, Y.F. Zhang, J.Q. Meng, Surface modification of cellulose membranes to prepare a high-capacity membrane adsorber for monoclonal antibody purification via hydrophobic charge-induction chromatography, Ind. Eng. Chem. Res. 57 (2018) 13235–13246.
[24] W.T. Riordan, S.M. Heilmann, K. Brorson, K. Seshadri, M.R. Etzel, Salt tolerant membrane adsorbers for robust impurity clearance, Biotechnol. Progr. 25 (2009) 1695–1702.
[25] M. Lin, N. Frau, R. Faber, A. Hesslein, J.H. Vogel, Polishing complex therapeutic proteins A new downstream purification platform using a salt-tolerant membrane adsorber, Biopharm. Int. 26 (2013) S14–S22.
[26] S.M. Lemma, C. Boi, R.G. Carbonell, Nonwoven ion-exchange membranes with high protein binding capacity for bioseparations, Membranes 11 (2021) 181.
[27] H.Y. Liu, P.V. Gurgel, R.G. Carbonell, Preparation and characterization of anion exchange adsorptive nonwoven membranes with high protein binding capacity, J. Membr. Sci. 493 (2015) 349–359.
[28] J. Fan, C. Boi, S.M. Lemma, J. Lavoie, R.G. Carbonell, Iminodiacetic acid (IDA) cation-exchange nonwoven membranes for efficient capture of antibodies and antibody fragments, Membranes 11 (2021) 15.
[29] G.H. Scholz, P. Wippich, S. Leistner, K. Huse, Salt-independent binding of antibodies from human serum to thiophilic heterocyclic ligands, J. Chromatogr. B 709 (1998) 189–196.
[30] H. Qian, Z.Y. Lin, H.M. Xu, M.Q. Chen, The efficient and specific isolation of the antibodies from human serum by thiophilic paramagnetic polymer nanospheres, Biotechnol. Progr. 25 (2009) 376–383.
[31] R.A. Lavoie, W.N. Chu, J.H. Lavoie, Z. Hetzler, T.I. Williams, R. Carbonell, S. Menegatti, Removal of host cell proteins from cell culture fluids by weak partitioning chromatography using peptide-based adsorbents, Sep. Purif. Technol. 257 (2021) 12.
[32] R.A. Lavoie, A. di Fazio, T.I. Williams, R. Carbonell, S. Menegatti, Targeted capture of Chinese hamster ovary host cell proteins: peptide ligand binding by proteomic analysis, Biotechnol. Bioeng. 117 (2020) 438–452.
[33] K. Wrzosek, M. Gramblicka, M. Polakovic, Influence of ligand density on antibody binding capacity of cation-exchange adsorbents, J. Chromatogr. A 1216 (2009) 5039–5044.
[34] A.M. Hardin, C. Harinarayan, G. Malmquist, A. Axen, R. van Reis, Ion exchange chromatography of monoclonal antibodies: effect of resin ligand density on dynamic binding capacity, J. Chromatogr. A 1216 (2009) 4366–4371.
[35] J.K. Rasmussen, C.A. Bothof, S.C. Atan, R.T. Fitzsimons, G.W. Griesgraber, J. I. Hembre, Ion exchange ligand design: improving membrane adsorber efficiencies by spacer arm manipulation, React. Funct. Polym. 136 (2019) 181–188.
[36] M.M. Zhu, G. Carta, Protein adsorption equilibrium and kinetics in multimodal cation exchange resins, Adsorpt.-J. Int. Adsorpt. Soc. 22 (2016) 165–179.
[37] Capto TM MMC ImpRes., Available online: https://gels.yilimart.com/Assets/Images/doc/file/17371601_DATAFILE_01.PDF.
[38] New selectivity and large design space for downstream purification processes, Available online: https://www.bio-rad.com/webroot/web/pdf/ps/literature/Bulletin_6242.pdf.
[39] Development of a high capacity, mixed-mode resin for high conductivity mAb feedstocks, Available online: https://bioprocessintl.com/2012/development-of-a-high-capacity-mixed-mode-resin-for-high-conductivity-mab-feedstocks-333720/.
[40] J. Yan, Q.L. Zhang, H.F. Tong, D.Q. Lin, S.J. Yao, Hydrophobic charge-induction resin with 5-aminobenzimidazol as the functional ligand: preparation, protein adsorption and immunoglobulin G purification, J. Sep. Sci. 38 (2015) 2387–2393.
[41] Y.Y. Li, Y. Sun, Poly(4-vinylpyridine): a polymeric ligand for mixed-mode protein chromatography, J. Chromatogr. A 1373 (2014) 97–105.
[42] J. Wang, R.T. Sproul, L.S. Anderson, S.M. Husson, Development of multimodal membrane adsorbers for antibody purification using atom transfer radical polymerization, Polymer 55 (2014) 1404–1411.
[43] J. Robinson, D. Roush, S.M. Cramer, The effect of pH on antibody retention in multimodal cation exchange chromatographic systems, J. Chromatogr. A 1617 (2020) 10.
[44] M.T. Li, X.J. Zou, Q.L. Zhang, D.Q. Lin, S.J. Yao, Binding mechanism of functional moieties of a mixed-mode ligand in antibody purification, Chem. Eng. J. 400 (2020) 8.
[45] M.A. Holstein, S. Parimal, S.A. McCallum, S.M. Cramer, Mobile phase modifier effects in multimodal cation exchange chromatography, Biotechnol. Bioeng. 109 (2012) 176–186.
[46] L.S. Wolfe, C.P. Barringer, S.S. Mostafa, A.A. Shukla, Multimodal chromatography: characterization of protein binding and selectivity enhancement through mobile phase modulators, J. Chromatogr. A 1340 (2014) 151–156.
[47] Y. Wan, T. Zhang, Y.M. Wang, Y. Wang, Y.F. Li, Removing light chain-missing byproducts and aggregates by Capto MMC ImpRes mixed-mode chromatography

during the purification of two WuXiBody-based bispecific antibodies, Protein Expr. Purif. 175 (2020) 10.
[48] T. Arakawa, Y. Kurosawa, M. Storms, T. Maruyama, C.J. Okumura, Y. Kita, Capto MMC mixed-mode chromatography of murine and rabbit antibodies, Protein Expr. Purif. 127 (2016) 105–110.
[49] M. Namazian, S. Halvani, Calculations of pKa values of carboxylic acids in aqueous solution using density functional theory, J. Chem. Thermodyn. 38 (2006) 1495–1502.
[50] H.R. Doss, M. Raman, R. Knihtila, N. Chennamsetty, D. Wang, A. Shupe, N. Mussa, Streamlining the polishing step development process via physicochemical characterization of monoclonal antibody aggregates, J. Chromatogr. A 1598 (2019) 101–112.
[51] A. Hirano, T. Maruyama, K. Shiraki, T. Arakawa, T. Kameda, Mechanism of protein desorption from 4-mercaptoethylpyridine resins by arginine solutions, J. Chromatogr. A 1373 (2014) 141–148.
[52] O. Khanal, V. Kumar, A.M. Lenhoff, Displacement to separate host-cell proteins and aggregates in cation-exchange chromatography of monoclonal antibodies, Biotechnol. Bioeng. 118 (2021) 164–174.
[53] J. Tang, X. Zhang, T. Chen, Y. Wang, Y. Li, Removal of half antibody, hole-hole homodimer and aggregates during bispecific antibody purification using MMC ImpRes mixed-mode chromatography, Protein Expres. Purif. 167 (2020), 105529.
[54] Y. Zhang, L. Cai, Y. Wang, Y. Li, Processing of high-salt-containing Protein A eluate using mixed-mode chromatography in purifying an aggregation-prone antibody, Protein Expres. Purif. 164 (2019), 105458.
[55] X.D. Zhang, T. Chen, Y.F. Li, A parallel demonstration of different resins' antibody aggregate removing capability by a case study, Protein Expr. Purif. 153 (2019) 59–69.
[56] C.L.Z. de Zafra, V. Quarmby, K. Francissen, M. Vanderlaan, J. Zhu-Shimoni, Host cell proteins in biotechnology-derived products: a risk assessment framework, Biotechnol. Bioeng. 112 (2015) 2284–2291.
[57] S.A. Sripada, W. Chu, T.I. Williams, M.A. Teten, B.J. Mosley, R.G. Carbonell, A. M. Lenhoff, S.M. Cramer, J. Bill, Y. Yigzaw, D.J. Roush, S. Menegatti, Towards continuous mAb purification: clearance of host cell proteins from CHO cell culture harvests via "flow-through affinity chromatography" using peptide-based adsorbents, Biotechnol. Bioeng. 119 (2022) 1873–1889.